

Prediction of Redox Potentials of Adrenaline and Its Supramolecular Complex with Glycine: Theoretical and Experimental Studies

Tao Liu,^{†,‡} Chunmei Du,[§] Zhangyu Yu,[§] Lingli Han,[‡] and Dongju Zhang^{*,†}

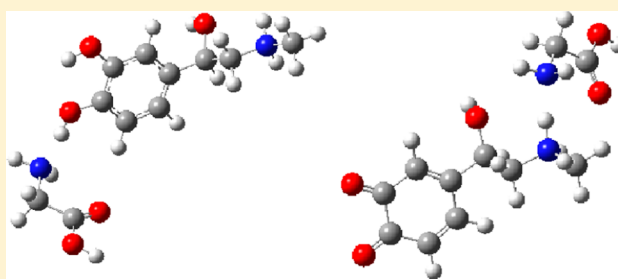
[†]Key Lab of Colloid and Interface Chemistry, Ministry of Education, Institute of Theoretical Chemistry, Shandong University, Jinan 250100, P. R. China

[‡]Key Laboratory of Inorganic Chemistry in Universities of Shandong, Department of Chemistry and Chemical Engineering, Jining University, Qufu 273155, P. R. China

[§]School of Chemistry and Chemical Engineering, Qufu Normal University, Qufu 273165, P. R. China

Supporting Information

ABSTRACT: Protonated adrenaline (PAd) can be oxidized to protonated adrenaline quinone (PAdquinone) through a one-step, two-electron redox reaction. The electron-transfer property of PAd and its supramolecular complex with glycine has been investigated by cyclic voltammetry (CV) experiment and theoretical calculations. From CV curves, the conditional formal redox potential $E^{\circ'}$ of PAd/PAdquinone couple at the pH value of 0.29 is determined to be 0.540 V. The calculated $E^{\circ'}$ using the G3MP2//B3LYP method and the B3LYP method with 6-31G(d,p), 6-31+G(d,p), 6-311G(d,p), and B3LYP/6-311+G(d,p) basis sets are in reasonable agreement with the experimental value. PAd can form supramolecular complex (PAd–Gly) with glycine (Gly) through hydrogen bond (H-bond), and the calculated $E^{\circ'}$ values of PAd–Gly/PAdquinone–Gly redox couple are larger than those of PAd/PAdquinone couple. The theoretical results are in good agreement with the experimental finding that the formation of H-bonds weakens the electron-donating ability of PAd.



1. INTRODUCTION

Electron-transfer reactions, which are considered to be a very active domain in natural science in recent years, play a vital role in chemistry and biology. The ability of a molecule to donate or accept an electron is determined by its standard redox potentials (E°), which is fundamental to understanding the innumerable chemical and biological electron-transfer reactions.^{1,2} E° data can be obtained directly from potentiometric measurements when the redox processes are reversible and quasi-reversible. Cyclic voltammetry (CV) is the most popular experimental method for measuring E° , which can provide a great deal of information about electrochemical systems and processes.^{3–5} However, for irreversible processes the experimental situation is complicated, and accurate E° values are available only via some sophisticated techniques such as pulse radiolysis.^{3–5} Therefore, it is not always easy to obtain reliable experimental E° data.¹

Given the limitation of the experimental methods, chemists have developed theoretical approaches calculating the standard redox potentials in solution. As seen in many publications,^{1,2,6–33} the electrode potentials of various chemical species have been predicted accurately by performing semi-empirical, density functional theory (DFT), and ab initio calculations. In particular, Tugsuz³³ performed an extensive DFT study of the standard electrode potentials of hydrogen-bonded (H-bonded) complexes by employing 10 hybrid density functionals. The calculated results indicate that DFT

methods can correctly predict standard electrode potentials of molecules and supramolecules.³³

Adrenaline is a hormone and neurotransmitter, which plays a particularly important role in the regulation of physiological processes in living systems.^{34,35} Adrenaline is not soluble in water and organic solvents, but can be dissolved in proton-donor solvents to form protonated adrenaline (PAd). PAd is unstable and is easily oxidized to form protonated adrenaline quinone (PAdquinone). PAd has important biological functions and can form supramolecular complexes with many biological molecules (e.g., amino acids) in the human body through intermolecular H-bond. Hence, it is necessary to develop an effective method to study electron-transfer processes for adrenaline and its supramolecular complexes.

To the best of our knowledge, there is no study on the prediction of redox potentials of PAd/PAdquinone and their supramolecular complexes. In the present work, we present a combined theoretical and experimental study to better understand the electron-transfer property of PAd and its supramolecular complexes. We first predict the redox potential of PAd/PAdquinone couple in aqueous solution through theoretical computations. Then, we investigate the electrochemical behavior PAd in the quasi-reversible redox processes

Received: December 3, 2012

Revised: January 26, 2013

Published: February 5, 2013



using the CV method, and test the validity of redox potential obtained by theoretical approaches. Finally, in order to understand the biological functions of PAd in the living systems, we select glycine (Gly) as a probe molecule to study the H-bond interaction between PAd and Gly. From calculated and experimental results, we study the change of the electrochemical behavior of PAd after the H-bond formation and predict the redox potentials of the H-bonded complexes (PAd–Gly and PAdquinone–Gly) by CV and theoretical calculation methods. The key aim of this work is to search an effective theoretical approach to predict the redox potential of adrenaline system exactly, and to determine the change of the electron-transfer property of PAd upon the H-bond formation. We expect that the present results would be useful for the prediction of electrode potentials of other molecules.

2. EXPERIMENTAL SECTION

The adrenaline reagent (>97%) was purchased from Fluka Co. (Sweden). The concentration of adrenaline aqueous solution was 5.0×10^{-3} mol L⁻¹. Other employed solutions were prepared with analytic grade reagents and doubly distilled water.

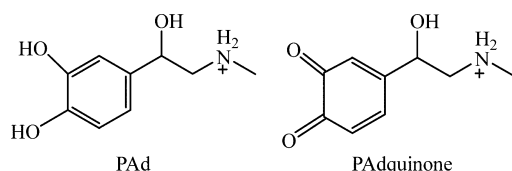
The electrochemical experiments were performed on an EG&G PAR M398 electrochemical impedance system with an M283 potentiostat/galvanostat. The three-electrode system was used to carry out electrochemical tests. Glassy carbon electrode (GCE) and Al₂O₃ modified glass carbon electrode (Al₂O₃/GCE)³⁶ served as working electrodes, a platinum wire served as a counter electrode, and a saturation calomel electrode (SCE) served as a reference electrode. A Luggin capillary was used to connect the reference and working electrodes in order to reduce the solution resistance. Highly pure nitrogen was passed through the solution for 15 min to remove dissolved oxygen in solution before measurements, and all measurements were carried out under nitrogen atmosphere at room temperature (298 K).

3. METHODS AND COMPUTATIONAL DETAILS

Different methods for calculating the standard electrode potentials have been developed by Namazian et al.,^{15,16} Kelly et al.,²⁷ and Song.³² In the present work, we use the following two methods to calculate the standard redox electrode potentials of PAd/PAdquinone and PAd–Gly/PAdquinone–Gly systems, as done in Tugsuz's work.³³ In these two methods, the redox potential is calculated via a thermochemical cycle.

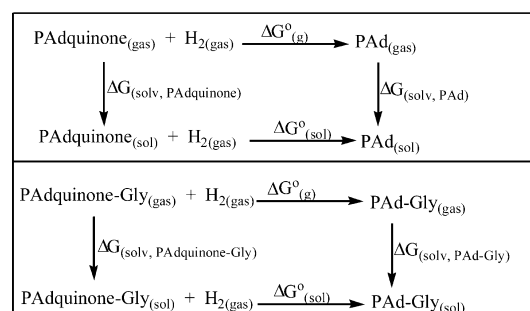
3.1. Method 1. Taking the PAd/PAdquinone redox couple as an example, we describe this method. PAd, as shown in Scheme 1, can be converted to its oxidized form PAdquinone through a two-electron-oxidation reaction in aqueous solution. The calculation of the redox electrode potential of PAd/PAdquinone couple, relative to the standard hydrogen electrode (SHE), is possible by calculating the Gibbs energy change of the following redox reaction

Scheme 1. Structures of PAd and PAdquinone



from the thermochemical cycle illustrated in the upper rectangle in Scheme 2. According to the cycle, $\Delta G_{(1)}^{\circ}$

Scheme 2. Proposed Thermochemical Cycle from Method 1



(subscript (1) means eq 1) can be calculated by the following equations

$$\Delta G_{(1)}^{\circ} = \Delta G_{(\text{g})}^{\circ} + \Delta G_{(\text{sol}, \text{PAd})} - \Delta G_{(\text{sol}, \text{PAdquinone})} \quad (2)$$

$$\Delta G_{(\text{g})}^{\circ} = \sum \nu_i G_{\text{g},i}^{\circ} \quad (3)$$

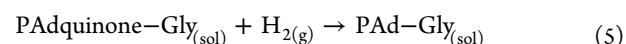
where $\Delta G_{\text{g},i}^{\circ}$ is the change of Gibbs free energy for each component in reaction 1.

The standard redox electrode potential of PAd/PAdquinone couple can be obtained by the following equation:

$$\Delta G_{(1)}^{\circ} = -nFE^{\circ} \quad (4)$$

where n is number of electrons transferred ($n = 2$ in the present case) and F is the Faraday constant (96485 C mol^{-1} or $23.061 \text{ kcal mol}^{-1} \text{ V}^{-1}$),³⁷ and E° is the standard redox electrode potential. It is noted that this method requires the reference electrode potential of SHE, which is equal 0.00 V in SI units.

The same method was employed to calculate the electrode potential of PAd–Gly/PAdquinone–Gly compared to SHE for the following reaction.



The change of the standard Gibbs energy of reaction 5 can be calculated according to the thermochemical cycle shown in the lower rectangle in Scheme 2, and hence the standard redox electrode potential of PAd–Gly/PAdquinone–Gly couple can be obtained.

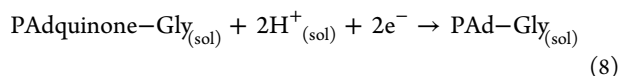
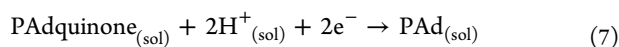
For reactions 1 and 5, the conditional formal redox potential, $E^{\circ'}$, can be obtained from the following equation

$$E^{\circ'} = E^{\circ} - (2.303mRT/2F)\text{pH} \quad (6)$$

where E° is the standard redox potential (or formal potential at pH = 0), m is the number of protons involved in the redox reactions ($m = 2$ in the present case), R is the gas constant, T is temperature, and F is Faraday constant. From eq 6, it can be seen that the conditional formal redox potentials of PAd/PAdquinone and PAd–Gly/PAdquinone–Gly couples are pH-dependent. With pH increasing, their conditional formal redox potentials will shift to negative values.

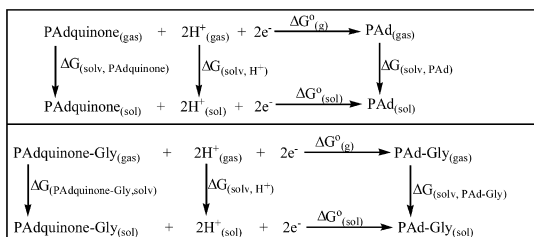
3.2. Method 2. In this method, the absolute redox potentials of PAd/PAdquinone and PAd–Gly/PAdquinone–Gly couples are calculated directly. PAd and PAd–Gly can be reduced from their oxidized forms, PAdquinone and

PAdquinone–Gly, respectively, via the following 2-electron half-reactions:



According to the thermochemical cycle shown in Scheme 3, $\Delta G^\circ_{(7),(8)}$ can be calculated from the following equations

Scheme 3. Proposed Thermochemical Cycle from Method 2



$$\Delta G^\circ_{(7)} = \Delta G^\circ_{(\text{g})} + \Delta G_{(\text{solv}, \text{PAd})} - \Delta G_{(\text{solv}, \text{PAdquinone})} - \Delta G_{(\text{solv}, \text{H}^+)} - n\Delta G^{\circ \rightarrow *} \quad (9)$$

$$\Delta G^\circ_{(8)} = \Delta G^\circ_{(\text{g})} + \Delta G_{(\text{solv}, \text{PAd–Gly})} - \Delta G_{(\text{solv}, \text{PAdquinone–Gly})} - \Delta G_{(\text{solv}, \text{H}^+)} - n\Delta G^{\circ \rightarrow *} \quad (10)$$

where n is number of electrons transferred ($n = 2$ in the present case), $\Delta G^{\circ \rightarrow *}$ is the correction for the change in standard state from 1 atm for gas-phase calculations “o” to 1 mol L^{−1} for solution phase “*”, which is 1.9 kcal mol^{−1} (or 7.9 kJ mol^{−1}) for each component ($RT \ln(24.46)$).³⁸ $\Delta G^\circ_{(\text{g})}$ can be obtained from eq 3.

In order to compare the calculated results with the experimental value, it is necessary to get the redox potentials of PAd/PAdquinone and PAd–Gly/PAdquinone–Gly couples relative to SHE. The absolute value of reduction potential of SHE is known to be 4.44 V.³⁷ Thus, the E° values of PAd/PAdquinone and PAd–Gly/PAdquinone–Gly versus SHE can be obtained, and the value of $E^{\circ'}$ can be calculated according to eq 6.

Note that from the equations involved in calculating ΔG° , it is obvious that the acidity of the solution will affect the Gibbs free energy change of the reaction. As described in the following section, the present calculations used water as solvent, and the solvation energies were estimated from a polarizable continuum medium model. Thus, no pH effect was taken into account actually. However, the effect of pH value on the ΔG° of a reaction is expected to be negligible because the calculated systematic errors on reactants and products will be counteracted mostly while calculating ΔG° .

3.3. Computational Details. The geometries of PAd, PAdquinone, PAd–Gly, and PAdquinone–Gly in the gas phase and aqueous solution were fully optimized within the framework of hybrid B3LYP functional^{39–42} with seven different basis sets. Harmonic vibrational frequencies were also calculated at the same level of theory to identify all stationary points as minima (zero imaginary frequencies). As pointed out by Wodrich et al.,⁴³ the B3LYP functional is sometimes not appropriate for obtaining accurate energies of

molecules. However, it has been established to be a reliable method for predicting the electrode potential of organic molecules.^{21,23,31,32} Here, to further evaluate the calculated results using the B3LYP functional, we also performed the benchmark calculations using both the high-level G3MP2//B3LYP⁴⁴ method and the BMK⁴⁵/TZVP⁴⁶ method, as recommended by Namazian²³ and Tugsuz,³³ respectively. It is found that the B3LYP results are in good agreement with those from the high-level G3MP2 calculations. Both the B3LYP and G3MP2//B3LYP methods reproduce the experimental observation for the conditional electrode potentials of PAd/PAdquinone redox couple, as will be seen in the section Results and Discussion. The solvation energies at the G3MP2//B3LYP level were estimated from the B3LYP/6-311+G(d,p) calculations.²³ In all calculations of solvation energies, we used the conductor-like polarizable continuum model (CPCM)^{47–49} with the UAHF radii as recommended by Namazian²⁰ and Frisch.⁵⁰ All the calculations were carried out using the Gaussian03 software⁵¹ package.

4. RESULTS AND DISCUSSION

4.1. Redox Electrode Potential of PAd/PAdquinone Couple. We obtained a series of $E^{\circ'}$ data by the theoretical calculations according to methods 1 and 2 described in section 3. To test the reliability of our theoretical calculations, we first determined the $E^{\circ'}$ value of the reversible processes via the CV method. The CV curves of 5.0×10^{-3} mol L^{−1} adrenaline at Al₂O₃/GCE in 0.5 M H₂SO₄ solution (pH = 0.29) are presented in Figure 1. There is a pair of quasireversible peaks in

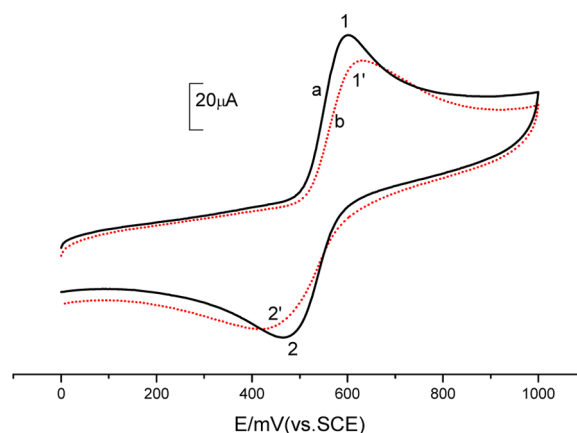


Figure 1. Cyclic voltammograms of 5×10^{-3} mol L^{−1} PAd in aqueous solution at Al₂O₃/GCE. The voltammograms are obtained in the solution with different concentration of Gly and using a scan rate of 50 mV/s. The lines (a) and (b) correspond to the Gly concentrations of 0 and 5×10^{-3} mol L^{−1}, respectively. The peak 1 (1′) denotes the anodic peak, and peak 2 (2′) denotes the cathodic peak.

curve (a), where peak 1 corresponds to the oxidation of PAd into PAdquinone (anodic peak), and peak 2 corresponds to the reduction of PAdquinone into PAd (cathodic peak). The conditional formal potential is approximated by the midpoint potential between the anodic and cathodic peaks, $E^{\circ'} = (E_{\text{pa}} + E_{\text{pc}})/2$, which has been used in many previous works.^{23,52} We have performed several groups of individual experiments to obtain a reliable experimental result. The mean value of the conditional formal potentials $E^{\circ'}$ determined from individual experiments for PAd/PAdquinone redox couple is 0.540 V with

Table 1. Calculated Gas-Phase Gibbs Energies $\Delta G_{g,i}^\circ$ and Solvation Energies $\Delta G_{\text{solv},i}$ of Studied Species at Different Levels of Theory

	PAd		PAdquinone		PAd–Gly		PAdquinone–Gly	
	G° (hartrees)	$\Delta G_{\text{solv}}^\circ$ (kcal mol ^{−1})	G° (hartrees)	$\Delta G_{\text{solv}}^\circ$ (kcal mol ^{−1})	G° (hartrees)	$\Delta G_{\text{solv}}^\circ$ (kcal mol ^{−1})	G° (hartrees)	$\Delta G_{\text{solv}}^\circ$ (kcal mol ^{−1})
G3MP2//B3LYP	−630.65773	−83.25	−629.40304	−103.51				
BMK/TZVP	−631.21654	−83.03	−629.97438	−101.72				
B3LYP/6-31G(d)	−631.37367	−78.17	−630.13680	−95.47				
B3LYP/6-31G(d,p)	−631.40923	−78.63	−630.16121	−96.31	−915.80444	−85.57	−914.57150	−92.83
B3LYP/6-31+G(d)	−631.39952	−83.21	−630.15920	−102.96				
B3LYP/6-31+G(d,p)	−631.43471	−83.37	−630.18303	−103.68	−915.84524	−92.01	−914.60641	−102.22
B3LYP/6-311G(d,p)	−631.56301	−80.65	−630.31284	−98.22	−916.03781	−87.84	−914.80198	−95.31
B3LYP/6-311+G(d,p)	−631.57670	−83.25	−630.32438	−103.51	−916.05968	−91.46	−914.82009	−100.03
B3LYP/6-311++G(2df,2p)	−631.61401	−77.45	−630.35989	−102.97				

Table 2. Gibbs Free Energies of the Studied Reactions, and the Theoretical and Experimental Electrode Potentials for the PAd/PAdquinone Redox Couple

	method 1			method 2			$E^{\circ'}(\text{V})$ (expt)
	$\Delta G_{(1)}^\circ$ (kcal mol ^{−1})	$E^\circ_1(\text{V})$ (calcd)	$E^{\circ'}_1(\text{V})$ (calcd)	$\Delta G_{(7)}^\circ$ (kcal mol ^{−1})	$E^\circ_2(\text{V})^a$ (calcd)	$E^{\circ'}_2(\text{V})^a$ (calcd)	
G3MP2//B3LYP	−25.62	0.555	0.538	−232.32	0.597	0.579	0.540
BMK/TZVP	−26.87	0.583	0.565	−226.02	0.460	0.443	
B3LYP/6-31G(d)	−20.38	0.442	0.424	−224.08	0.418	0.401	
B3LYP/6-31G(d,p)	−25.10	0.544	0.527	−230.70	0.562	0.544	
B3LYP/6-31+G(d)	−20.10	0.436	0.419	−230.93	0.567	0.550	
B3LYP/6-31+G(d,p)	−24.76	0.537	0.520	−230.37	0.555	0.538	
B3LYP/6-311G(d,p)	−25.84	0.560	0.543	−232.16	0.594	0.576	
B3LYP/6-311+G(d,p)	−24.50	0.531	0.514	−230.82	0.565	0.547	
B3LYP/6-311++G(2df,2p)	−20.10	0.436	0.418	−226.70	0.475	0.458	

^aThe value is relative to the potential of SHE.

pH value of 0.29. Thus, the corresponding standard redox electrode potential E° is 0.557 V.

The most stable structures of PAd and PAdquinone optimized in aqueous solution optimized at the G3MP2//B3LYP level are shown in Figure S1 of the Supporting Information. Table 1 shows the calculated gas-phase Gibbs energies $\Delta G_{g,i}^\circ$ and solvation energies $\Delta G_{\text{solv},i}$ for PAd and PAdquinone, calculated at nine different theoretical levels. The total changes in Gibbs free energy for reactions 1 and 7, $\Delta G_{(1)}^\circ$ and $\Delta G_{(7)}^\circ$, the standard redox electrode potential $E^\circ(\text{calcd})$, and the conditional formal potential $E^{\circ'}(\text{calcd})$ for PAd/PAdquinone redox couple using methods 1 and 2 are given in Table 2, where the experimental conditional formal potential $E^{\circ'}(\text{expt})$ is also listed for comparison. Calculated Gibbs free energies $\Delta G_{g,i}^\circ$ of H_2 are given in Table S1 in the Supporting Information. According to the calculated gas-phase energies together with the CPCM solvation energies, we can obtain the conditional formal potential $E^{\circ'}$ for reactions 1 and 7.

As shown in Table 2, the calculated $E^{\circ'}$ values for PAd/PAdquinone redox couple obtained at the G3MP2//B3LYP, BMK/TZVP, B3LYP/6-31G(d,p), B3LYP/6-31+G(d,p), B3LYP/6-311G(d,p), and B3LYP/6-311+G(d,p) levels with method 1 are in reasonable agreement with the experimental value of 0.54 V (deviations are less than 0.05 V). Among them, $E^{\circ'}$ values at the G3MP2//B3LYP and B3LYP/6-31G(d,p) levels show a very small deviation (0.002 and 0.003 V) in comparison with the experimental value. However, it should be noted that the values of the redox potential at the B3LYP/6-311++G(2df,2p) level are underestimated remarkably. On the

other hand, using method 2 the results calculated using the G3MP2//B3LYP method and the B3LYP method with the 6-31G(d,p), 6-31+G(d), 6-31+G(d,p), 6-311G(d,p), and 6-311+G(d,p) basis sets are reasonably close to the experimental value, and the deviations are 0.039, 0.004, 0.010, 0.002, 0.036, and 0.007 V, respectively. It is also noted that, although the result (0.565 V) from the BMK/TZVP calculations using method 1 is also close to the experimental value with deviation of 0.025 V, the corresponding value (0.443 V) obtained using method 2 is underestimated obviously.

From the results above, it is clear that for PAd/PAdquinone redox couple the G3MP2//B3LYP method and the B3LYP method with the 6-31G(d,p), 6-31+G(d,p), 6-311G(d,p), and 6-311+G(d,p) basis sets give the reliable results. The corresponding deviations are 0.002, 0.013, 0.020, 0.003, and 0.026 V in method 1, and 0.039, 0.004, 0.002, 0.036, and 0.007 V in method 2. The results demonstrate that the optimal five levels of theory are accurate enough to predicate the electrode potential of PAd/PAdquinone redox couple. In subsequent calculations for PAd–Gly/PAdquinone–Gly redox couple, considering the limitation of computational resources, we only performed the B3LYP calculations with the 6-31G(d,p), 6-31+G(d,p), 6-311G(d,p), and B3LYP/6-311+G(d,p) basis sets.

4.2. Electrode Potential of PAd–Gly/PAdquinone–Gly Redox Couple. The CV curve of 5.0×10^{-3} mol L^{−1} PAd and Gly with molar ratio of 1:1 at $\text{Al}_2\text{O}_3/\text{GCE}$ in 0.5 M H_2SO_4 solution (pH = 0.29) is shown in the curve (b) of Figure 1. It can be seen that with the addition of Gly, the electron-donating ability of PAd decreases: the anodic peak potential shifts

positively ($1 \rightarrow 1'$), the anodic peak potential shifts negatively ($2 \rightarrow 2'$), the peak-to-peak potential separation between anodic and anodic peak potential increases, and the anodic and anodic peak current decreases significantly. The results demonstrate the inhibition effect of Gly on the electron-donating ability of PAd. The supramolecular complex of PAd–Gly formed through H-bond interaction between PAd and Gly can slow down the diffusion ability of adrenaline and make PAd hard to be oxidized.

Before calculating the electrode potentials of PAd–Gly/PAdquinone–Gly redox couple, it is helpful to have a thorough knowledge of the geometries of complexes PAd–Gly and PAdquinone–Gly, since the thermochemical values are controlled by molecular geometries. It should be noted that PAd can form supramolecular complex with Gly at different ratios, while in this section, we only discuss the stable structure of 1:1 supramolecular complex. The structures of the supramolecular complexes of PAd/PAdquinone with Gly were obtained by geometry optimization calculations. The initial geometries of the complexes were obtained by attaching Gly to the different positions of PAd and PAdquinone, including the phenolic hydroxyl, alcoholic hydroxyl, and amino group.

Figure 2 shows the most stable H-bonded complexes PAd–Gly and PAdquinone–Gly in aqueous solution optimized at the

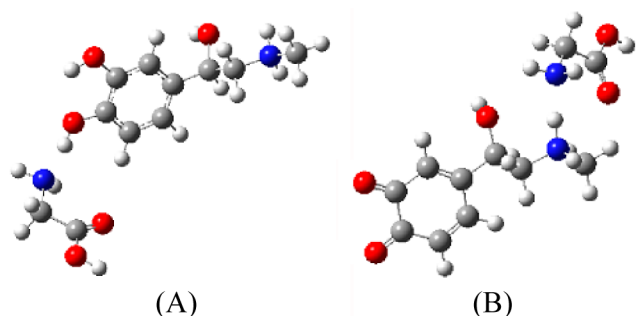


Figure 2. The most stable H-bonded complexes PAd–Gly and PAdquinone–Gly, optimized in aqueous solution at the B3LYP/6-311+G(d,p) level.

B3LYP/6-311+G(d,p) level. It is found that in these two complexes the H-bond acceptor is the nitrogen atom in Gly, while the H-bond donors are the phenolic hydroxyl group in PAd for complex PAd–Gly and the amino group in PAdquinone for complex PAdquinone–Gly. The complex geometries obtained using the 6-31G(d,p), 6-31+G(d,p), and

6-311G(d,p) basis sets are very similar to that from the 6-311+G(d,p) basis set. Table 3 displays the geometric parameters of the H-bond parts in the PAd–Gly complex optimized at these levels of theory, and also lists the calculated H-bond interaction energies in the gas phase and aqueous solution. As shown in Table 3, upon the formation of H-bond, the O–H bond lengths in PAd–Gly complex in the gas phase and aqueous solution are longer compared to those in free PAd. The $H_{\text{PAd}} \cdots N_{\text{Gly}}$ distance values are within a range between 1.647 and 1.750 Å and the $O_{\text{PAd}}-H_{\text{PAd}} \cdots N_{\text{Gly}}$ angles are larger than 169.7° in the two phases. The calculated H-bond interaction energies (-19.21 , -16.48 , -18.80 , and -15.91 kcal mol $^{-1}$) for complex PAd–Gly in the gas phase are significantly larger than those (-10.41 , -6.50 , -9.75 , and -6.02 kcal mol $^{-1}$) in solution.

In Table 3, we also compared the calculated O–H bond stretching vibrational frequencies in PAd–Gly and PAd. It is found that the O–H bond vibrational mode in PAd–Gly is shifted toward higher frequency compared to that in PAd. For example, the O–H stretching mode calculated at B3LYP/6-311+G(d,p) are red-shifted by 789 and 769 cm $^{-1}$ in the gas phase and in aqueous solution, respectively. This is attributed to the fact that the formation of the H-bond weakens the O–H bond.

The calculated H-bond parameters for complex PAdquinone–Gly are shown in Table S2 in the Supporting Information. The H-bond character in PAdquinone–Gly is similar to that in complex PAd–Gly, so we do not discuss them again.

The gas-phase Gibbs energies $\Delta G_{\text{g},i}^\circ$ and solvation energies $\Delta G_{\text{solv},i}$ for the complexes PAd–Gly and PAdquinone–Gly are listed in Table 1. The calculated ΔG° , E° , and $E^{\circ'}$ for the PAd–Gly/PAdquinone–Gly redox couple using methods 1 and 2 are given in Table 4. With method 1, $E^{\circ'}$ values at the pH value of 0.29 calculated using the B3LYP functional with the 6-31G(d,p), 6-31+G(d,p), 6-311G(d,p), and 6-311+G(d,p) basis sets are 0.550, 0.564, 0.567, and 0.597 V, respectively. With method 2, the corresponding values are 0.565, 0.582, 0.600, and 0.628 V.

Comparing the calculated $E^{\circ'}$ values in Table 2 with those in Table 4, we find that the theoretical $E^{\circ'}$ value for the PAd–Gly/PAdquinone–Gly redox couple calculated using both the methods is always larger than that for the PAd/PAdquinone redox couple, which indicates that the formation of H-bonds weaken the electron-donating ability of PAd. The result is consistent with the CV experiment that Gly hinders PAd

Table 3. Geometric Parameters^{a,b} of the $O_{\text{PAd}}-H_{\text{PAd}} \cdots N_{\text{Gly}}$ Parts in Complex PAd–Gly in the Gas Phase and in Aqueous Solution,^c the Frequencies (in cm $^{-1}$) for the Stretching Vibration of the O–H bond of PAd, and the H-bond Interaction Energies (ΔE , in kcal/mol) in the Complexes

	$R(\text{O}-\text{H})$	$R(N_{\text{Gly}} \cdots H_{\text{PAd}})$	$\angle O_{\text{PAd}}H_{\text{PAd}} \cdots N_{\text{Gly}}$	frequencies	ΔE
B3LYP/6-31G(d,p)	1.010 (0.966) ^d	1.709	171.1	2971 (3832) ^e	-19.21
	1.021 (0.981)	1.661	170.6	2724 (3512)	-10.41
B3LYP/6-31+G(d,p)	1.009 (0.967)	1.723	169.8	2978 (3831)	-16.48
	1.027 (0.983)	1.647	170.8	2621 (3479)	-6.50
B3LYP/6-311G(d,p)	1.003 (0.963)	1.734	170.7	3036 (3836)	-18.80
	1.016 (0.978)	1.676	170.6	2762 (3502)	-9.75
B3LYP/6-311+G(d,p)	1.003 (0.964)	1.750	169.7	3046 (3835)	-15.91
	1.019 (0.979)	1.675	170.7	2715 (3484)	-6.02

^aFor labeling, see Figure 2A. ^bBond lengths are given in Å, and angles in degrees. ^cThe values in solution are denoted in italics. ^dValues in parentheses are the bond lengths in the free PAd. ^eValues in parentheses are the O–H bond stretching frequencies in the free PAd.

Table 4. Gibbs Free Energy of the Studied Reactions, and Redox Potentials of PAd–Gly/PAdquinone–Gly Calculated with Methods 1 and 2 at Different Levels of Theory

	method 1			method 2		
	$\Delta G^\circ_{(s)}$ (kcal mol ^{−1})	E°_1 (V) (calcd)	$E^{\circ'}_1$ (V) (calcd)	$\Delta G^\circ_{(s)}$ (kcal mol ^{−1})	E°_2 (V) ^a (calcd)	$E^{\circ'}_2$ (V) ^a (calcd)
B3LYP/6-31G(d,p)	−26.05	0.565	0.550	−231.66	0.583	0.565
B3LYP/6-31+G(d,p)	−26.80	0.581	0.564	−232.41	0.599	0.582
B3LYP/6-311G(d,p)	−26.94	0.584	0.567	−233.27	0.618	0.600
B3LYP/6-311+G(d,p)	−28.20	0.611	0.597	−234.52	0.645	0.628

^aThe value is relative to the potential of SHE.

oxidization to PAdquinone, which can be attributed to the fact that Gly forms H-bond with the hydrogen atom of phenolic hydroxyl group in PAd as shown in Figure 2A. The formed H-bond can protect the phenolic hydroxyl groups of PAd, reduce the electron-donating ability of PAd, and make it hard to be oxidized.

Our theoretical calculations rationalize the experimental observation well and reproduce the experimental redox potential for the irreversible electrode process. The present study indicates that the B3LYP functional combined with appropriate basis sets can predict correct electrode potentials of PAd/PAdquinone and PAd–Gly/PAdquinone–Gly redox couples. The calculation methods established here are expected to be also available for investigating the interaction between PAd and other biological molecules.

5. CONCLUSIONS

In the present work, the electron-donating ability of PAd and its supramolecular complex with Gly has been investigated by CV and theoretical calculation methods. PAd is oxidized to PAdquinone through a one-step, two-electron redox reaction. The conditional formal redox potential $E^{\circ'}$ at the pH value of 0.29 is found to be 0.540 V through the CV experiment. The calculated $E^{\circ'}$ value for the PAd/PAdquinone redox couple using the G3MP2//B3LYP method and the B3LYP functional combined with the 6-31G(d,p), 6-31+G(d,p), 6-311G(d,p), and 6-311+G(d,p) basis sets are in reasonable agreement with the experimental value. The CV experiment demonstrates the electron-donating ability of PAd decreases with the H-bond formation between PAd and Gly. The calculated $E^{\circ'}$ values for the PAd–Gly/PAdquinone–Gly redox couple using the B3LYP functional combined with the 6-31G(d,p), 6-31+G(d,p), 6-311G(d,p), and 6-311+G(d,p) basis sets are larger than those for the PAd/PAdquinone redox couple. The results show that the formation of H-bonds weakens the electron-donating ability of PAd. There is good agreement between the experimental and theoretical studies.

■ ASSOCIATED CONTENT

Supporting Information

The optimized most stable structures of PAd and PAdquinone in aqueous solution, the geometric parameters and H-bond interaction energies in PAdquinone–Gly, and the calculated gas-phase Gibbs energies of H₂. This material is available free of charge via the Internet at <http://pubs.acs.org>.

■ AUTHOR INFORMATION

Corresponding Author

*E-mail: zhangdj@sdu.edu.cn.

Notes

The authors declare no competing financial interest.

■ ACKNOWLEDGMENTS

This work was jointly supported by National Natural Science Foundation of China (No. 21273131), the Natural Science Foundation of Shandong Province (No. ZR2009BM003), China Postdoctoral Science Foundation Funded Project (No. 2011MS00724), and Shandong Province Postdoctoral Innovation Foundation Funded Project China (No. 201102019).

■ REFERENCES

- (1) Fu, Y.; Liu, L.; Yu, H. Z.; Wang, Y. M.; Guo, Q. X. *J. Am. Chem. Soc.* **2005**, *127*, 7227–7234.
- (2) Fu, Y.; Liu, L.; Wang, Y. M.; Li, J. N.; Yu, T. Q.; Guo, Q. X. Quantum Chemical Predictions of Redox Potentials of Organic Anions in Dimethyl Sulfoxide and Reevaluation of Bond Dissociation Enthalpies Measured by the Electrochemical Methods. *J. Phys. Chem. A* **2006**, *110*, 5874–5886.
- (3) Bard, A. J.; Faulkner, L. R. *Electrochemical Methods: Fundamentals and Applications*; Wiley: New York, 2001.
- (4) Hamann, C. H.; Hamnett, A.; Vielstich, W. *Electrochemistry*; Wiley-VCH: New York, 1998.
- (5) Wishart, J. F.; Nocera, D. G., Eds.; *Photochemistry and Radiation Chemistry: Complementary Methods for the Study of Electron Transfer*; American Chemical Society: Washington, DC, 1998.
- (6) Rzepa, H. S.; Suñer, G. A. Theoretical Calculations of Benzoquinone Redox Potentials Using the COSMO Continuum Solvation Model. *J. Chem. Soc., Chem. Commun.* **1993**, 1743–1744.
- (7) Wheeler, R. A. Method for Computing One-Electron Reduction Potentials and Its Application to p-Benzoquinone in Water at 300 K. *J. Am. Chem. Soc.* **1994**, *116*, 11048–11051.
- (8) Raymond, K. S.; Grafton, A. K.; Wheeler, R. A. Calculated One-Electron Reduction Potentials and Solvation Structures for Selected p-Benzoquinones in Water. *J. Phys. Chem. B* **1997**, *101*, 623–631.
- (9) Jalali-Heravi, M.; Namazian, M.; Peacock, T. E. Theoretical Studies of Electrode Potentials in Aqueous Solution. Investigation of Individual Contributions from Electrostatic, Cavity and Dispersion Interactions to Redox Potentials. *J. Electroanal. Chem.* **1995**, *385*, 1–8.
- (10) Jalali-Heravi, M.; Namazian, M. Optimization of the Cavity Size for AM1-SCRF Calculations of Electrode Potentials in Aqueous Solution. *J. Electroanal. Chem.* **1997**, *425*, 139–146.
- (11) Fontanesi, C.; Benassi, R.; Giovanardi, R.; Marcaccio, M.; Paolucci, F.; Roffia, S. Computational Electrochemistry. Ab Initio Calculation of Solvent Effect in the Multiple Electroreduction of Polypyridinic Compounds. *J. Mol. Struct.* **2002**, *612*, 277–286.
- (12) Namazian, M.; Norouzi, P.; Ranjbar, R. Prediction of Electrode Potentials of Some Quinone Derivatives in Acetonitrile. *J. Mol. Struct. (THEOCHEM)* **2003**, *625*, 235–241.
- (13) Namazian, M. Density Functional Theory Response to the Calculation of Electrode Potentials of Quinones in Non-Aqueous Solution of Acetonitrile. *J. Mol. Struct. (THEOCHEM)* **2003**, *664–665*, 273–278.
- (14) Namazian, M.; Norouzi, P. Prediction of One-Electron Electrode Potentials of Some Quinones in Dimethylsulfoxide. *J. Electroanal. Chem.* **2004**, *573*, 49–53.

- (15) Namazian, M.; Almodarresieh, H. A. Computational Electrochemistry: Aqueous Two-electron Reduction Potentials for Substituted Quinines. *J. Mol. Struct. (THEOCHEM)* **2004**, 686, 97–102.
- (16) Namazian, M.; Almodarresieh, H. A.; Noorbala, M. R.; Zare, H. R. DFT Calculation of Electrode Potentials for Substituted Quinones in Aqueous Solution. *Chem. Phys. Lett.* **2004**, 396, 424–428.
- (17) Namazian, M.; Zare, H. R. Electrochemistry of Chlorogenic Acid: Experimental and Theoretical Studies. *Electrochim. Acta* **2005**, 50, 4350–4355.
- (18) Zare, H. R.; Namazian, M.; Nasirizadeh, N. Electrochemical Behavior of Quercetin: Experimental and Theoretical Studies. *J. Electroanal. Chem.* **2005**, 584, 77–83.
- (19) Namazian, M.; Zare, H. R. Computational Electrode Potential of a Coumestan Derivative: Theoretical and Experimental Studies. *Biophys. Chem.* **2005**, 117, 13–17.
- (20) Namazian, M.; Coote, M. L. Accurate Calculation of Absolute One-Electron Redox Potentials of Some Para-Quinone Derivatives in Acetonitrile. *J. Phys. Chem. A* **2007**, 111, 7227–7232.
- (21) Namazian, M.; Zare, H. R.; Coote, M. L. Determination of the Absolute Redox Potential of Rutin: Experimental and Theoretical Studies. *Biophys. Chem.* **2008**, 132, 64–68.
- (22) Zare, H. R.; Eslami, M.; Namazian, M.; Coote, M. L. Experimental and Theoretical Studies of Redox Reactions of o-Chloranil in Aqueous Solution. *J. Phys. Chem. B* **2009**, 113, 8080–8085.
- (23) Eslami, M.; Zare, H. R.; Namazian, M. Thermodynamic Parameters of Electrochemical Oxidation of L-DOPA: Experimental and Theoretical Studies. *J. Phys. Chem. B* **2012**, 116, 12552–12557.
- (24) Namazian, M.; Zare, H. R.; Coote, M. L. Theoretical Study of the Oxidation Mechanism of Hematoxylin in Aqueous Solution. *Aust. J. Chem.* **2012**, 65, 486–489.
- (25) Winget, P.; Weber, E. J.; Cramer, C. J.; Truhlar, D. G. Computational Electrochemistry: Aqueous One-Electron Oxidation Potentials for Substituted Anilines. *Phys. Chem. Chem. Phys.* **2000**, 2, 1231–1239.
- (26) Winget, P.; Cramer, C. J.; Truhlar, D. G. Computation of Equilibrium Oxidation and Reduction Potentials for Reversible and Dissociative Electron-Transfer Reactions in Solution. *Theor. Chem. Acc.* **2004**, 112, 217–227.
- (27) Kelly, C. K.; Cramer, C. J.; Truhlar, D. G. Single-ion Solvation Free Energies and the Normal Hydrogen Electrode Potential in Methanol, Acetonitrile, and Dimethyl Sulfoxide. *J. Phys. Chem. B* **2007**, 111, 408–422.
- (28) Dutton, A. S.; Fukuto, J. M.; Houk, K. N. Theoretical Reduction Potentials for Nitrogen Oxides from CBS-QB3 Energetics and (C)PCM Solvation Calculations. *Inorg. Chem.* **2005**, 44, 4024–4028.
- (29) Wass, J. R. T. J.; Ahlberg, E.; Panas, I.; Schiffrin, D. J. Quantum Chemical Modeling of the Reduction of Quinones. *J. Phys. Chem. A* **2006**, 110, 2005–2020.
- (30) Frontana, C.; Vázquez-Mayagoitia, Á.; Garza, J.; Vargas, R.; González, I. Substituent Effect on a Family of Quinones in Aprotic Solvents: an Experimental and Theoretical Approach. *J. Phys. Chem. A* **2006**, 110, 9411–9419.
- (31) Haya, L.; Sayago, F. J.; Mainar, A. M.; Cativielab, C.; Urieta, J. S. Quantum-Chemical Predictions of Redox Potentials of Carbamates in Methanol. *Phys. Chem. Chem. Phys.* **2011**, 13, 17696–17703.
- (32) Song, Y. Z. Theoretical Studies on Electrochemistry of p-aminophenol. *Spectrochim. Acta A* **2007**, 67, 611–618.
- (33) Tugsuz, T. DFT Study on the Standard Electrode Potentials of Imidazole, Tetrathiafulvalene, and Tetrathiafulvalene-Imidazole. *J. Phys. Chem. B* **2010**, 114, 17092–17101.
- (34) Hawley, M. D.; Tatawawadi, S. V.; Piekarski, S.; Adams, R. N. Electrochemical Studies of the Oxidation Pathways of Catecholamines. *J. Am. Chem. Soc.* **1967**, 89, 447–450.
- (35) Cui, H.; Wu, L.; Chen, J.; Lin, X. Multi-Mode in Situ Spectroelectrochemical Studies of Redox Pathways of Adrenaline. *J. Electroanal. Chem.* **2001**, 504, 195–200.
- (36) Liu, T.; Yu, Z. Y. Experimental and Theoretical Study on the Supramolecular Complexes of 15-Crown-5 with Adrenaline. *Bioorg. Med. Chem. Lett.* **2010**, 20, 4845–489.
- (37) Bard, A. J.; Faulkner, L. R. *Electrochemical Methods: Fundamentals and Applications*; Wiley: New York, 2001.
- (38) Liptak, M. D.; Gross, K. C.; Seybold, P. G.; Feldgus, S.; Shields, G. C. Absolute pKa Determinations for Substituted Phenols. *J. Am. Chem. Soc.* **2002**, 124, 6421–6427.
- (39) Becke, A. D. Density - Functional Thermochemistry. III. The Role of Exact Exchange. *J. Chem. Phys.* **1993**, 98, 5648–5653.
- (40) Miehlich, B.; Savin, A.; Stoll, H.; Preuss, H. Results Obtained with the Correlation Energy Density Functionals of Becke and Lee, Yang and Parr. *Chem. Phys. Lett.* **1989**, 157, 200–206.
- (41) Lee, C.; Yang, W.; Parr, G. Development of the Colle-Salvetti Correlation-Energy Formula into a Functional of the Electron Density. *Phys. Rev. B* **1988**, 37, 785–789.
- (42) Stephens, P. J.; Devlin, F. J.; Chabalowski, C. F. Ab Initio Calculation of Vibrational Absorption and Circular Dichroism Spectra Using Density Functional Force Fields. *J. Phys. Chem.* **1994**, 98, 11623–11627.
- (43) Wodrich, M. D.; Corminboeuf, C.; Schreiner, P. R.; Fokin, A. A.; Schleyer, P. v. R. How Accurate Are DFT Treatments of Organic Energies? *Org. Lett.* **2007**, 9, 1851–1854.
- (44) Anantharaman, B.; Melius, C. F. Bond Additivity Corrections for G3B3 and G3MP2B3 Quantum Chemistry Methods. *J. Phys. Chem. A* **2005**, 109, 1734–1747.
- (45) Boese, A. D.; Martin, J. M. L. Development of Density Functionals for Thermochemical Kinetics. *J. Chem. Phys.* **2004**, 121, 3405–3417.
- (46) Schaefer, A.; Huber, C.; Ahlrichs, R. Fully Optimized Contracted Gaussian Basis Sets of Triple Zeta Valence Quality for Atoms Li to Kr. *J. Chem. Phys.* **1994**, 100, 5829–5836.
- (47) Barone, V.; Cossi, M. Quantum Calculation of Molecular Energies and Energy Gradients in Solution by a Conductor Solvent Model. *J. Phys. Chem. A* **1998**, 102, 1995–2001.
- (48) Cossi, M.; Rega, N.; Scalmani, G.; Barone, V. Energies, Structures, and Electronic Properties of Molecules in Solution with the C-PCM Solvation Model. *J. Comput. Chem.* **2003**, 24, 669–681.
- (49) Takano, Y.; Houk, K. N. Benchmarking the Conductor-like Polarizable Continuum Model (CPCM) for Aqueous Solvation Free Energies of Neutral and Ionic Organic Molecules. *J. Chem. Theor. Comput.* **2005**, 1, 70–77.
- (50) Frisch, A. E.; Frisch, M. J.; Trucks, G. W. *Gaussian 03 User's references*; Gaussian, Inc.: Carnegie, PA, 2003.
- (51) Frisch, M. J.; Trucks, G. W.; Schlegel, H. B.; Scuseria, G. E.; Robb, M. A.; Cheeseman, J. R.; Montgomery, J. A., Jr.; Vreven, T.; Kudin, K. N.; Burant, J. C.; Millam, J. M.; Iyengar, S. S.; Tomasi, J.; Barone, V.; Mennucci, B.; Cossi, M.; Scalmani, G.; Rega, N.; Petersson, G. A.; Nakatsuji, H.; Hada, M.; Ehara, M.; Toyota, K.; Fukuda, R.; Hasegawa, J.; Ishida, M.; Nakajima, T.; Honda, Y.; Kitao, O.; Nakai, H.; Klene, M.; Li, X.; Knox, J. E.; Hratchian, H. P.; Cross, J. B.; Bakken, V.; Adamo, C.; Jaramillo, J.; Gomperts, R.; Stratmann, R. E.; Yazyev, O.; Austin, A. J.; Cammi, R.; Pomelli, C.; Ochterski, J. W.; Ayala, P. Y.; Morokuma, K.; Voth, G. A.; Salvador, P.; Dannenberg, J. J.; Zakrzewski, V. G.; Dapprich, S.; Daniels, A. D.; Strain, M. C.; Farkas, O.; Malick, D. K.; Rabuck, A. D.; Raghavachari, K.; Foresman, J. B.; Ortiz, J. V.; Cui, Q.; Baboul, A. G.; Clifford, S.; Cioslowski, J.; Stefanov, B. B.; Liu, G.; Liashenko, A.; Piskorz, P.; Komaromi, I.; Martin, R. L.; Fox, D. J.; Keith, T.; Al-Laham, M. A.; Peng, C. Y.; Nanayakkara, A.; Challacombe, M.; Gill, P. M. W.; Johnson, B.; Chen, W.; Wong, M. W.; Gonzalez, C.; Pople, J. A. *Gaussian 03, revision A.1*; Gaussian, Inc.: Pittsburgh, PA, 2004.
- (52) Wang, J. *Analytical Electrochemistry*, 2nd ed.; John Wiley & Sons: New York, 2000.